2024 IEEE International Conference on Robotics and Automation (ICRA 2024)
May 13-17, 2024. Yokohama, Japan

A Deep Learning Framework for Non-Symmetrical Coulomb Friction Identification of Robotic Manipulators

M. Lahoud[1,2], G. Marchello[1], M. D'Imperio[1], A. Müller[3], F. Cannella[1]

Abstract— **The determination of the dynamic properties of a robot is especially important for designing highly accurate and efficient control systems. Conventional methods for dynamic model identification have proven to be effective, where deep learning (DL) approaches have shown limits due to data inefficiencies. However, thanks to novel physics-informed DL architectures, such as Deep Lagrangian Networks (DeLaN) [1], it is possible to control and extract interpretable physical information of a robot. This paper introduces an augmented DeLaN architecture for linear viscous and non-symmetrical Coulomb friction identification, which also learns motor parameters such as rotor inertia. An approach is proposed for comparing this method with the conventional dynamic identification and previous DeLaN implementations. Moreover, our friction and rotor inertia identification is validated, and the performance of our model is analyzed with a real robot (UR5e).**

I. INTRODUCTION

Accurate dynamic parameter identification enhances model-based controller effectiveness in robot control. Many authors have dealt with the estimation of said parameters by deriving the Inverse Dynamic Identification Model (IDIM) from the Lagrange-Euler formulation and then solving an overdetermined system by using Least Squares (LS) [2]–[4]. A distinct demand emanating from the fundamental physics of robotic models is that the system inertia matrix must exhibit the properties of symmetry and positive definiteness. In this matter, Gautier *et al.* provided a systematic and efficient method to include such requirements into the mathematical solution [5]. In this way, by using singular value decomposition, Cholesky factorization and IDIM-LS technique for identification of the dynamic parameters of robots, they obtained a symmetric and positive definite inertia matrix. Moreover, LS techniques have proven to accomplish their task for serial, parallel and even humanoid robot architectures. Jubien *et al.* illustrated the applicability of their approach in the context of a redundant 7-degree-of-freedom serial manipulator [6]. Their resulting approach was able to reverse engineer the dynamic parameters of the manufacturer with the exception of the stiffness of the robot. Additionally, on complex robot architectures such as parallel robots, Briot *et al.* demonstrated the effectiveness of the LS approach on a physical Orthoglide parallel robot [4]. On top of that, they successfully identified the drive gains of the actuators.

On the other hand, novel methods including the use of complex Machine Learning (ML) methods, such as Deep Learning (DL) networks or hybrid approaches are recently being used for model identification and control [7]–[11]. The earliest ML-based techniques for modelling dynamics without requiring any physically interpretable parameters are usually referred to as black-box models. Conventional methods for dynamic parameter identification utilize comprehensive robot geometric, kinematic, and dynamic data [8]. Conversely, black-box methods only need input-output data of the system to estimate its condition for the following time-step. In consequence, their lack of learning toward solutions that correspond to physical systems causes them to be data inefficient [10] and of limited applicability for certain control techniques (*e.g.*, computed torque and passivity-based control).

As an alternative learning solution that matches physical systems, Lutter *et al.* proposed a Lagrangian mechanics-informed DL network, named Deep Lagrangian Network (DeLaN) [1]. DeLaN, is capable of estimating the inertia matrix and the potential energy of the robotic system at a given state. In contrast with conventional methods, this approach ensures the symmetry and positive definitiveness of its mass matrix, while learning. Additionally, DeLaN has proven to work on systems in which the total mechanical energy (the sum of potential and kinetic energies) remains constant over time, *i.e.*, conservative systems. However, in order to make use of this approach on non-conservative ones, two main strategies can be exploited:

1) DeLaN + blackbox for friction: this hybrid DL methodology was introduced by Gupta et al. [10] and combines the use of a DeLaN architecture with a *Dissipative Force Network*. Their method employs a black-box model to capture input-dependent non-conservative forces and other independent dissipative forces. DeLaN, enabled model-based controllers, but the lack of interpretable friction values limits architecture usability for system identification.

2) DeLaN + Linear Friction Models: Lutter *et al.* presented a DeLaN architecture considering friction forces [7], [8]. The assumption of frictions as linear networks dependant of the generalized coordinates enables DeLaN to infer the friction coefficients as networks weights. In such a way, they could identify viscous, Coulomb and stribeck friction parameters.

Conventional as well as DL-based approaches for parameter identification, both LS and DeLaN methods require

[1]M. Lahoud, G. Marchello, M. D'Imperio and F. Cannella are with Industrial Robotics Facility, Italian Institute of Technology, Via Morego 30, 16163 Genoa, Italy (marcel.lahoud, gabriele.marchello, mariapaola.dimperio, ferdinando.cannella)@iit.it

[2]M. Lahoud is with DIBRIS, University of Genoa. Genoa, Italy marcel.lahoud@edu.unige.it

[3]A. Müller is with the Institute of Robotics, Johannes Kepler University. Linz, Austria a.mueller@jku.at

measurement/training data. In particular, they exploit data from the robot joints, such as joint torque, position, velocity and acceleration while executing amplitude- and frequency-rich trajectories, known as *excitation trajectories* [5], [6], [12]. These trajectories are conventionally obtained through an optimization process, based on the IDIM, so that the the dynamical parameters are best exited. Comparably, DeLaN benefits as well of persistent excitation trajectories [1] using cosine trajectories, as they result in dynamic movements. Nonetheless, in previous works, persistence of the excitation trajectories for training DeLaN was not addressed. Moreover, there is still no proper standard or optimal method for generating trajectories that can deliver valuable dynamic information to the DL models.

The main contributions of this paper are 1) a DL method for directly discern the non-symmetric Coulomb friction (NSCF) and 2) the rotor inertia of the motors. Facilitating complex behavior modeling in DL-based robot dynamic identification, thus contributing to robotic calibration and identification, and 3) the analysis of conventionally generated persistent trajectories and their impact in the learning process of our method. In order to validate our approach, experiments in a real robot (UR5e) are conducted, and the goal of this work is to investigate whether DL methodologies can be used as a data-efficient and trustworthy method to accurately identify and control intricate mechanical systems, *e.g.* robots.

The paper comprises five sections. Section II outlines the conventional and DeLaN robotic dynamic model identification formulation. Section III details the methodology, encompassing the proposed DeLaN architecture and the synthesis of training and testing excitation trajectories. Section IV covers the experimental testing on our rig and the resulting methodology outcomes. Lastly, Section V encompasses the discussion, conclusions, and future work suggestions.

II. DYNAMICS FORMULATION

The formulation for conventional robotic dynamic identification and DeLaN has it roots in the same Lagrangian formalism. This formulation considers that the equations of motion for any mechanical system can be described in terms of the generalized coordinates by:

$$\boldsymbol{\tau} = \frac{d}{dt}\frac{\partial \mathcal{L}}{\partial \dot{\boldsymbol{q}}} - \frac{\partial \mathcal{L}}{\partial \boldsymbol{q}} \tag{1}$$

where $\boldsymbol{\tau}$ is the vector of generalized forces exerted on the system, $\boldsymbol{q}$ is the vector of generalized coordinates, that for rigid robots simplifies to the same joint coordinate, $\dot{\boldsymbol{q}}$ is the vector of generalized velocities and $\mathcal{L}$ is the *Lagrangian*. Moreover, the *Lagrangian* is considered as the difference between kinetic and potential energy. Additionally, the kinetic energy can be expressed in terms of the inertia matrix of the system or in terms of the sum of the generalized inertia ($\boldsymbol{M}_j$) and Jacobian (${}^{j}\boldsymbol{J}_j$) matrices of the *j*-th body.

$$\boldsymbol{E} = \frac{\dot{\boldsymbol{q}}^T \boldsymbol{M}(\boldsymbol{q})\dot{\boldsymbol{q}}}{2} = \frac{\dot{\boldsymbol{q}}^T \sum_j \left({}^{j}\boldsymbol{J}_j^T(\boldsymbol{q})\boldsymbol{M}_j\, {}^{j}\boldsymbol{J}_j(\boldsymbol{q}) \right) \dot{\boldsymbol{q}}}{2} \tag{2}$$

Furthermore, one can represent the potential energy as the sum of the potential energy of the *j*-th body in the base frame. Hence, it can be articulated in terms of the vector of gravitational acceleration, the transformation matrix from the base frame to the *j*-th body frame, and the vector of the first moment of inertia and the mass of the *j*-th body.

$$\boldsymbol{U} = \sum_j U_j = -\begin{bmatrix} {}^{0}\boldsymbol{g}^T & 0 \end{bmatrix} \sum_j \left({}^{0}\boldsymbol{T}_j(\boldsymbol{q}) \begin{bmatrix} {}^{j}\boldsymbol{ms}_j \\ m_j \end{bmatrix} \right) \tag{3}$$

where $\boldsymbol{g}^T$ is the transposed vector of gravitational acceleration, and $\boldsymbol{ms}_j$ and m_j are the first moment of inertia vector and the mass of the *j*-th body, respectively. Hence, by developing (1) using (3) and (2), yields

$$\boldsymbol{\tau} = \boldsymbol{M}(\boldsymbol{q})\ddot{\boldsymbol{q}} + \dot{\boldsymbol{M}}(\boldsymbol{q})\dot{\boldsymbol{q}} - \frac{\left(\frac{\partial}{\partial \boldsymbol{q}}\left(\dot{\boldsymbol{q}}^T \boldsymbol{M}(\boldsymbol{q})\dot{\boldsymbol{q}}\right)\right)^T}{2} + \boldsymbol{G}(\boldsymbol{q}) \tag{4}$$

which models the equation of motion of the mechanical system in the form of a second-order differential equation. However, when considering non-conservative forces such as friction, motor inertia or external wrenches, in the case these are generalized forces [1] (*i.e.* they can be expressed in function of generalized coordinates), it is possible to sum them in the left-hand side of (4). Hence, (4) is typically presented in the literature in the next form:

$$\boldsymbol{\tau} = \boldsymbol{M}(\boldsymbol{q})\ddot{\boldsymbol{q}} + \boldsymbol{C}(\boldsymbol{q}, \dot{\boldsymbol{q}})\dot{\boldsymbol{q}} + \boldsymbol{G}(\boldsymbol{q}) + \boldsymbol{\tau}_f + \boldsymbol{\tau}_{ext} \tag{5}$$

where $\boldsymbol{M}(\boldsymbol{q})$ is the inertia matrix, $\boldsymbol{C}(\boldsymbol{q}, \dot{\boldsymbol{q}})$ is the Coriolis and centrifugal effects matrix, $\boldsymbol{G}(\boldsymbol{q})$ are the gravitational effects, $\boldsymbol{\tau}_f$ are the friction forces and $\boldsymbol{\tau}_{ext}$ are the external torques. Moreover, the total friction forces are typically the sum of the viscous and the Coulomb effects $\boldsymbol{\tau}_f = \boldsymbol{\tau}_v + \boldsymbol{\tau}_c$ [13].

$$\boldsymbol{\tau}_f = diag(\boldsymbol{f}_v)\dot{\boldsymbol{q}} + diag(\boldsymbol{f}_c)sign(\dot{\boldsymbol{q}}) + \boldsymbol{\tau}_{off} \tag{6}$$

where $\boldsymbol{f}_v$ and $\boldsymbol{f}_c$ represent the vector of viscous and Coulomb friction parameters, and $\boldsymbol{\tau}_{off}$ the vector of torque offsets from amplifiers and non-symmetric Coulomb friction. In this paper, the effects of torques resulting from external wrenches were not considered.

A. Conventional Robotic System Identification

Conventional robotic system identification methods are based on the Lagrange formalism. It considers the fact that there is a set of parameters called *standard parameters* that holds a linear relation with the kinetic and potential energy. Moreover, incorporating non-conservative forces into the model as a function of the generalized coordinates enhances model complexity and allows for considering motor and friction parameters. The vector of *standard dynamic parameters* is defined as $\boldsymbol{\chi}_j^T = [\Theta_j, I_j, \Phi_j]$ where Θ_j are the inertial parameters associated to the *j*-th body axial moments and cross-moments of inertia, the first moment of inertia and the mass $[xx_j,\ xy_j,\ xz_j,\ yy_j,\ yz_j,\ zz_j,\ mx_j,\ my_j,\ mz_j,\ m_j]$; I_j are the motor parameters $[Ia]$; and Φ_j are the friction parameters $[fv_j,\ fc_j,\ \tau_{off_j}]$.

Hence, developing the Lagrangian formulation in (1) and taking into account the linear relations of the dynamic parameters with the energy equations, the regressor matrix

$\boldsymbol{W}(\boldsymbol{q}, \dot{\boldsymbol{q}}_a, \ddot{\boldsymbol{q}}_a)$ is derived. This matrix relates the input efforts $\boldsymbol{\tau}$ to the dynamic parameters

$$\boldsymbol{\tau} = \boldsymbol{W}(\boldsymbol{q}, \dot{\boldsymbol{q}}_a, \ddot{\boldsymbol{q}}_a)\boldsymbol{\chi}_{st} \tag{8}$$

this implies that by measuring torques and computing the $\boldsymbol{W}$ matrix from the estimated robot state, these dynamic parameters can be determined.

Given that joint torques and joint states are measured at a frequency of fm, the outcome is a vector comprising the measured torque values $\boldsymbol{Y}_{fm}(\boldsymbol{\tau})$, a matrix of observations $\boldsymbol{W}^{st}_{fm}(\hat{\boldsymbol{q}}_a, \hat{\dot{\boldsymbol{q}}}_a, \hat{\ddot{\boldsymbol{q}}}_a)$ and a vector of errors $\boldsymbol{\rho}_{fm}$. Subsequently, the acquired data undergoes additional processing through filtering and re-sampling procedures. This sequence of steps guarantees a full-rank observation matrix by adjusting the standard parameters based on the foundational parameters.

$$\boldsymbol{Y}(\boldsymbol{\tau}) = \boldsymbol{W}^b(\hat{\boldsymbol{q}}_a, \hat{\dot{\boldsymbol{q}}}_a, \hat{\ddot{\boldsymbol{q}}}_a)\boldsymbol{\chi}_b + \boldsymbol{\rho} \tag{9}$$

Hence, the LS solution of $\boldsymbol{\chi}_b$ yields $\boldsymbol{\chi}_b = \boldsymbol{W}^{+}\boldsymbol{Y}$

B. DeLaN + Linear Friction Models

DeLaN, takes inspiration from the Lagrangian mechanics formalism. This type of physics-informed neural network estimates the inertia matrix of the system $\hat{\boldsymbol{M}}(\boldsymbol{q};\theta)$ and the potential energy $\hat{\boldsymbol{U}}(\boldsymbol{q};\psi)$ by using a DL network. Moreover, the estimation of the inertia matrix of the system in the form of a Cholesky decomposition plus a positive regularization offset ϵ guarantees the positive definiteness of $\hat{\boldsymbol{M}}$ [8] *i.e.*,

$$\hat{\boldsymbol{M}}(\boldsymbol{q};\theta) = \hat{\boldsymbol{L}}(\boldsymbol{q};\theta)\hat{\boldsymbol{L}}(\boldsymbol{q};\theta)^T + \epsilon \boldsymbol{I} \tag{10}$$

Then, the network parameters (θ and ψ) are learned while minimizing the error between the predicted torques $\hat{\boldsymbol{\tau}}(\boldsymbol{q}, \ddot{\boldsymbol{q}}, \ddot{\boldsymbol{q}}; \theta, \psi)$ from (4) and the measured torques $\boldsymbol{\tau}$.

$$(\theta^*, \psi^*) = \arg\min_{\theta,\psi} \ell\left(\hat{\boldsymbol{\tau}}(\boldsymbol{q}, \ddot{\boldsymbol{q}}, \ddot{\boldsymbol{q}}; \theta, \psi), \boldsymbol{\tau}\right) + \lambda\Omega(\theta, \psi) \tag{11}$$

where $\lambda\Omega(\theta, \psi)$ is a weight decay regularization, which should improve the learning of a unique solution of $\mathcal{L}$. During the training stage, the network learns to predict the torque values while estimating the system inertia matrix and the potential energy. Consequently, by modelling said models as linear networks, it is possible to learn the coefficients (f_v, f_c) as network weights. However, the NSCF phenomena and the rotor inertia of the motors have never been taken into consideration with this method.

III. METHODOLOGY

A. Proposed DeLaN architecture

As mentioned in section II-B, model identification can be done through DeLaN. Moreover, with the knowledge that linear models can be represented as linear networks and their coefficients learnt as the network weights [7]. DeLaN+NSCF exploits the contributions of the original DeLaN for infering the mass matrix and the potential energy of the robot. Furthermore, DeLaN computes the contributions of the conservative forces as represented in the dashed block in *Fig.* 1a. In addition, with the ideas exposed in [7] and [8], an augmented DeLaN architecture that models non-conservative forces as linear networks to learn the rotor inertia I_a, the viscous friction f_v and the non-symmetric Coulomb friction f_c^+, f_c^- is proposed. DeLaN+NSF includes a new component shown in the dashed-dotted square in *Fig.*a 1. Through our proposed architecture, the symmetrical viscous parameters are learned through a single linear network $\boldsymbol{f}_v$ which takes the inputs from the joint velocities $\dot{\boldsymbol{q}}$ and outputs its contribution to $\boldsymbol{\tau}_f$. Furthermore, in the particular case of learning the non-symmetrical Coulomb friction coefficients, the identification is split up into two linear networks $\boldsymbol{f}_c^+$ and $\boldsymbol{f}_c^-$, which takes inputs from the sign of $\dot{\boldsymbol{q}}$, modeled as $tanh(100\dot{\boldsymbol{q}})$. Consequently, the output of the network $\boldsymbol{f}_c^+$ is multiplied by $+1$ and then passed through a ReLu in order to sum its contribution to $\boldsymbol{\tau}_f$, yet only in one sense of the joints rotations. In a similar way, the output of $\boldsymbol{f}_c^-$ is multiplied by -1 and then passed through a ReLu to sum its contribution to $\boldsymbol{\tau}_f$ considering in this way the opposite direction of the previous outputs. In addition, it was considered a linear network for the rotor inertia ($\boldsymbol{I_a}$), as these are linear with respect to the acceleration of the robot joints. Consequently, the contributions of $\boldsymbol{\tau}_f$ and $\boldsymbol{\tau}_{I_a}$ are feed to the torque estimation, and through the minimization of the loss function during training, the dynamic parameters are learnt.

B. Generation of excitation trajectory

The quality of the model estimation method is linked to the excitation of the dynamics of the robot through persistent trajectories [14], [15]. It was proposed to use trajectories derived from the conventional method, to allow for a fair comparison with our approach. Hence, by minimizing the condition number of the regressor matrix it is possible to guarantee that the trajectories were optimally persistent and the identification results to be comparable for both the conventional and our approach. Finite Fourier series were used to represent the excitation trajectories

$$q_i(t) = \sum_{l=1}^{N_i} \frac{a_l^i}{\omega_f l} sin(\omega_f l t) - \frac{b_l^i}{\omega_f l} cos(\omega_f l t) + q_{i0}$$
$$\dot{q}(t) = \sum_{l=1}^{N_i} a_l^i cos(\omega_f l t) - b_l^i sin(\omega_f l t)$$
$$\ddot{q}(t) = \sum_{l=1}^{N_i} -a_l^i \omega_f l sin(\omega_f l t) - b_l^i \omega_f l cos(\omega_f l t)$$

where $q(t), \dot{q}(t)$ and $\ddot{q}(t)$ are joints position, velocity and acceleration, respectively. Furthermore, ω_f is the fundamental frequency and N_i is the number of harmonics of the Fourier series. Consequently, a_l^i and b_l^i are the amplitude parameters for the sine and cosine waves, respectively.

Therefore, the trajectories were obtained by minimizing the cost function defined by the condition number and the smallest singular value (σ_{min}) of the regressor matrix of the robot as in [16]

$$\begin{aligned} \min_{a,b} \quad & \lambda_1 cond(\mathbf{W}^T\mathbf{W}) + \frac{\lambda_2}{\boldsymbol{\sigma}_{min}} \\ \text{s.t.} \quad & Z_{min} \leq Z \leq Z_{max} \\ & [\boldsymbol{q}, \dot{\boldsymbol{q}}, \ddot{\boldsymbol{q}}]_{min} \leq [\boldsymbol{q}, \dot{\boldsymbol{q}}, \ddot{\boldsymbol{q}}] \leq [\boldsymbol{q}, \dot{\boldsymbol{q}}, \ddot{\boldsymbol{q}}]_{max} \end{aligned}$$

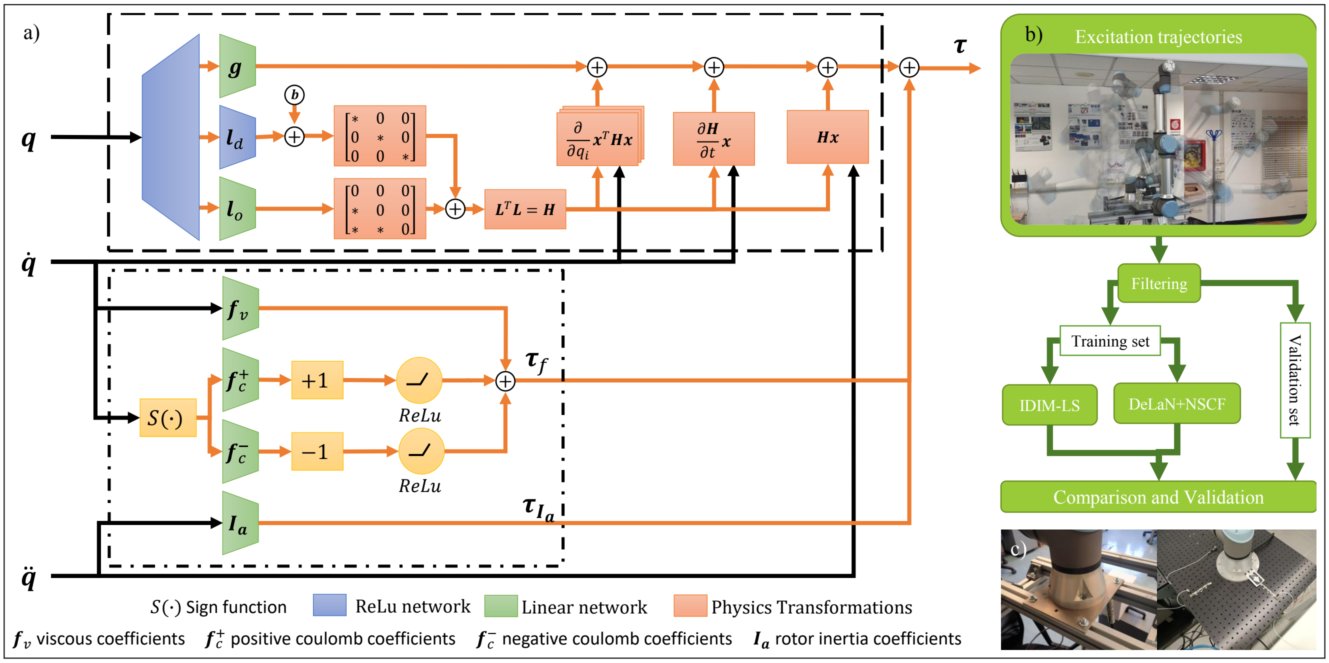

Fig. 1. a) Proposed DL-architecture for dynamics identification incluiding viscous and non-symmetrical Coulomb friction. The dashed square corresponds to the DeLaN architecture developed by Lutter et al. [1]. The dash-dotted square corresponds to the architecture developed by us for estimation of viscous and non-symmetrical Coulomb friction coefficients assuming linear models. b) Graphical representation of the methodology used to compare the IDIM-LS method and the proposed DL-method. c) Anchorings of the robot base. The first picture presents the anchoring using a structural rig made of Aluminum profile 8 40x40. The second picture displays the anchoring of the UR5e robot to the anti-vibration table.

where λ_1 and λ_2 are gains defined by the user to assign weights on the effect of each criterion in the cost function.

IV. RESULTS

A DL architecture based on DeLaN able to capture friction and inertial forces, such as the NSCF and rotor inertia has been presented. Since there are still no standard criteria for optimal excitation trajectory generation for DL-based identification, the decision was made to use those from section III-B with the aim of comparing both methodologies from the same starting point.

A. Robot tests

In order to compare the performance of our DeLaN+NSCF for dynamic identification with the conventional IDIM-LS method, a UR5e manufactured by Universal Robots was used. Moreover, for the trajectory generation and conventional IDIM-LS identification it was used the BIRDy framework [16] developed by Leboutet *et al.*

By starting from the knowledge of the kinematic and workspace restrictions of our robot, the conventional method of excitation trajectory generation was deployed. A set of 46 feasible excitation trajectories 10 s long each and sampled at 500 Hz was obtained. Then, these trajectories were executed on the robot, as depicted in *Fig.* 1b, using the ur_rtde libraries from SDU robotics on an Ubuntu PC running on a real-time kernel. While performing these excitation trajectories, joint position, velocity and current were measured. Consequently, 5th order Butterworth filters with a cut-off frequency of 10 Hz and a sampling border of 300 were applied to the measured data. Hence, these filtered trajectories were used as dataset for training and validation of the proposed architecture. Thus, 6 random trajectories out of the 46 total were excluded to be reserved for later validation purposes. Consequently, for all our models we considered training and validation loss to prevent overfitting. Therefore, the resulting IDIM-LS model was obtained through the mean value of the estimated parameters of all the 40 trajectories in the training dataset. The DeLaN+NSCF model was trained on an NVIDIA RTX3090 GPU installed on a Ubuntu PC. Furthermore, in order to assess the efficiency of the dynamic parameters learning, the model was trained six times while using 10, 20, 40, 60, 80, and 100 percent of the training set.

The robot manufacturer does not make the dynamic parameters of the robot public (in particular the friction parameters). Therefore, the validation of DeLaN+NSCF was done by comparing with respect to the IDIM-LS technique. Consequently, the validation phase of this work consisted in studying the relative differences of the friction and motor inertia coefficient identification. Subsequently, the analysis of the absolute differences in the torque decomposition results of our model with respect to the conventional IDIM-LS method. And, the comparison of torque estimation performance of IDIM-LS, DeLaN (with only viscous and symmetric Coulomb friction) and ours DeLaN+NSCF to unseen trajectories. Furthermore, these metrics were carried out on two different UR5e robots as depicted in *Fig.* 1c. One UR5e robot was mounted on a structure made of aluminum Profile 8 40x40 (referred to as No Vib-Free), and a second UR5e was mounted on an anti-vibration table (referred to as Vib-Free). Such a process, backed up with the conventional identification would validate our architecture. Moreover, this method would help to evaluate the performance of DeLaN+NSCF with regards to IDIM-LS and original DeLaN

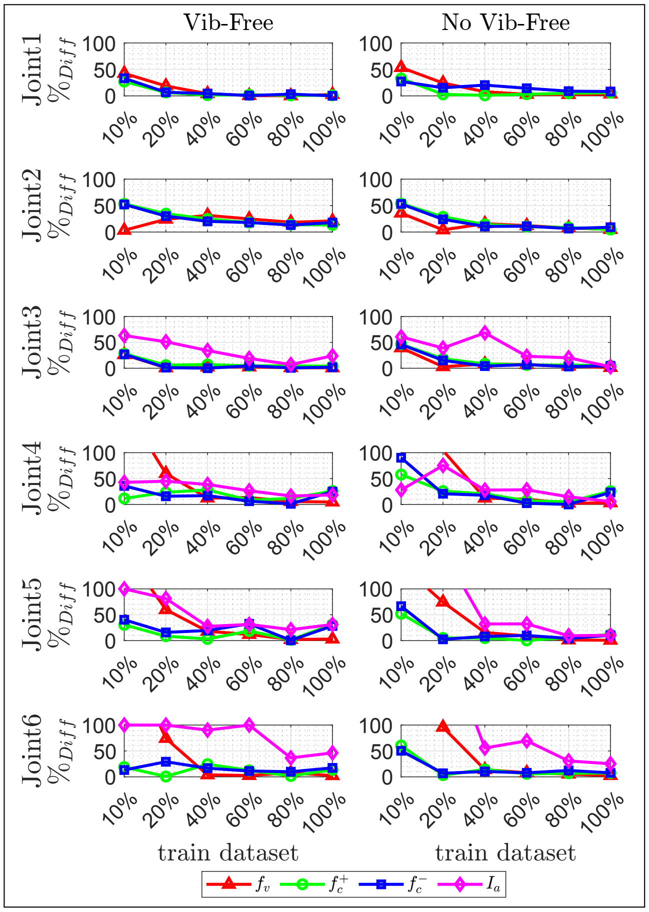

Fig. 2. Relative differences of the parameter identification of the proposed DeLaN+NSCF trained on different dataset sizes with respect to the mean values of the conventional IDIM-LS identification for each joint of the UR5e. Each column presents the resulting relative differences of the tests with and without vibration compensation (Vib-Free and No Vib-Free, respectively).

TABLE I
MEAN SQUARED ERROR PERFORMANCE OF THE **IDIM-LS**, THE ORIGINAL **DELAN** AND **DELAN+NSCF** FOR BOTH TESTS

	Validation trajectories MSE					
	1	2	3	4	5	6
IDIM-LS (No Vib-free)	5.10	3.58	**3.25**	5.59	4.24	4.41
DeLaN (No Vib-free)	41.84	28.60	28.02	40.35	28.45	35.29
DeLaN+NSCF (No Vib-free)	5.34	3.58	3.27	6.26	4.55	5.56
IDIM-LS (Vib-free)	**2.74**	**2.99**	3.96	**3.56**	**2.76**	**3.21**
DeLaN (Vib-free)	8.23	9.09	8.72	13.41	10.20	11.87
DeLaN+NSCF (Vib-free)	3.29	3.45	4.47	4.92	3.13	5.81

implementation. Additionally, both tests conditions would give us information on how the method performs under different anchoring situations.

B. Results

Consequently, after performing the training process, the relative difference between the identified parameters of DeLaN+NSCF with those of the IDIM-LS method through different train dataset sizes were compared, as depicted in *Fig.* 2. As expected, it was observed that for most of the parameters, the training size helped the network to deduce the parameters and reduce the relative difference with the parameters of the IDIM-LS. Consequently, our DL-architecture was able to identify the friction coefficients of the tested mechanical system, including those of the NSCF. The viscous friction for all the training dataset sizes was identified. For the entire training dataset, it was found that at the 40% mark of the training set, in both experiments, the tendency was to narrow the difference with respect to the IDIM-LS identification.

Continuing with the identification of friction coefficients for both experiences, in the NSCF parameters $\boldsymbol{f}_c^+$ and $\boldsymbol{f}_c^-$, small relative differences to the IDIM-LS were also observed. In particular, for training set sizes bigger than 40%. However, when arriving to the 100% of the training set, the fourth joint presented up to 25% difference for both tests. Moreover, joint five presented up to 30% difference at 100% of the training set in the experiments done with the anti-vibration table. Conversely, it was observed that the identification of the rotor inertia $\boldsymbol{I}_a$ of the motors benefits from the size of the training dataset. Even though, rotor inertia of joints 1 and 2 were identified using DeLaN+NSCF, it was not possible to compare because in the IDIM-LS solution these parameters did not belong to the vector of base parameters.

Overall, the observed tendency was that the bigger the training data set was, the resulting difference between our method and the conventional IDIM-LS method became smaller. This tendency was also true for the torque predictions of our model. Moreover, thanks to the torque decomposition capabilities of DeLaN, it was possible to examine closely the errors in all the elements of (5) and analyze the results on *Fig.* 3 for the second validation trajectory. In the first row of *Fig.* 3 it is observed that the error behaviour on torque prediction of our method is quite similar to that of the conventional identification on the filtered signals. Subsequently, rows 2 to 5 depict the difference between the torque components between the IDIM-LS model and our DeLaN+NSCF model, respectively. By observing rows 2 to 5, it can be seen that a performance very close to a conventional IDIM-LS was achieved by our trained model. In particular the difference in friction identification in the six joints helps to validate our model for NSCF identification. Furthermore, the effects on the difference of the inferred friction parameters with respect to the conventional methods are evident in the discontinuities of $\hat{\boldsymbol{\tau}}_f$ Moreover, the tests done with the robot mounted on a anti-vibration table gave better performances.

Additionally, the analysis of the mean squared error (MSE) performance in table I allowed us to to understand better the performance of our model to the unseen validation trajectories and to close the validation of our implementation. Additionally, we include the results from a DeLaN model that considered only symmetrical viscous and Coulomb frictions. Even though, for both the tests the MSE of our model did not performed better than the IDIM-LS method. It should be noted that the performance of our method is comparable to that of the conventional method. Furthermore, it performed better than a DeLaN that considered only symmetrical friction models. Consequently, considering the parameter identification and the torque prediction results compared to the conventional ones, our implementation can be validated as a viable approach for DL dynamic identifi-

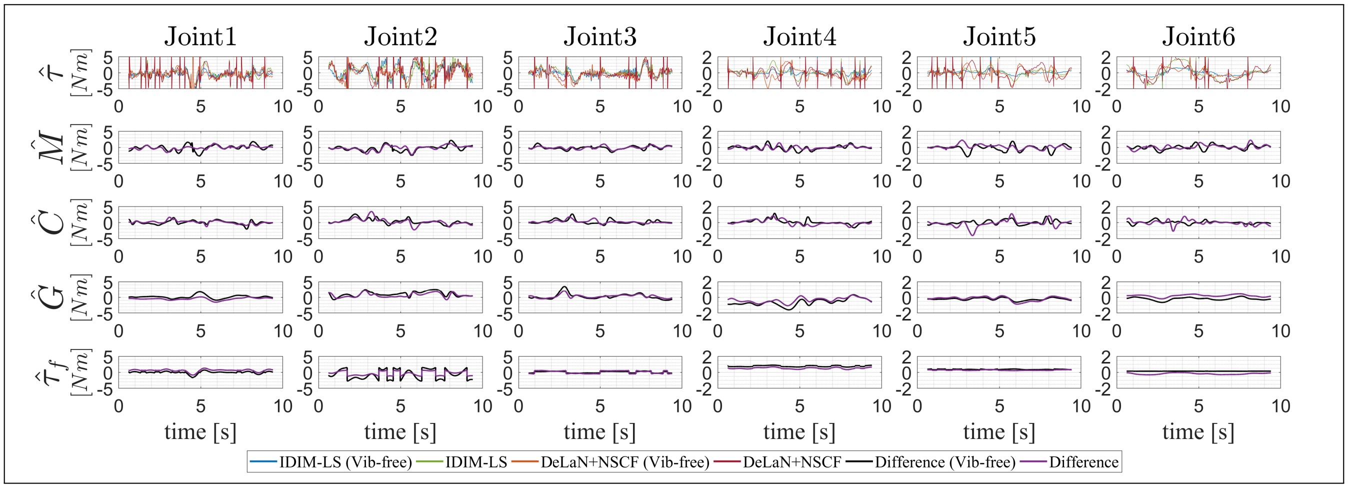

Fig. 3. Torque comparative analysis of the models trained on 100% of the training dataset estimating torques of the second validation trajectory. In the first row the blue and green lines represents the absolute error between the IDIM-LS estimated torques and the filtered torques for each test, respectively. While, the red and orange lines represents the absolute errors between DeLaN+NSCF and the filtered torques for each test, respectively. Furthermore, rows 2 to 5 depicts the differences between the conventional method and ours in the individual components that constitute the equation of motion of the robot. The black and purple lines represents the mentioned differences on the robot with and without damping compensation, respectively.

cation.

V. DISCUSSION AND CONCLUSION

A. Discussion

This study presented and validated a method for robot dynamic identification using a white-box DL approach, addressing new key challenges such as NSCF and rotor inertia. Moreover, the effect of using optimal excitation trajectories demonstrated useful for the parameter and overall identification of the robot dynamics using our method. Thanks to the increased model complexity of our approach, the performance was better than the previous approach that considered only symmetrical friction models as it was evidenced in table I. Furthermore, the positive effect of the anchoring of the robot base to an anti-vibration table is observed in the overall performance of all the models. Additionally, the robustness of the DL method to non-linearities is highlighted, since the performance improvements are not as different as those present in the conventional method. This fact, could make our approach to be practical in particular cases, such as floating base systems, *e.g.* a robot manipulator mounted on a mobile robot. A better performance than the IDIM-LS was not expected as the identification trajectories are optimized for the conventional method, and our method does not consider all the geometric, kinematic and dynamic equations of the robot. Nonetheless, the results suggests that the performance could still be improved and this could be achieved through the learning nature of our method.

B. Conclusion

This work at the best of the authors knowledge is the first one to introduce the linear NSCF model to a DL method for robot dynamic identification. Taking into account that an accurate dynamic model is crucial for model-based controllers, through our validation and comparative analysis, our DeLaN+NSCF demonstrated its potentialities for parameter identification and torque estimation on a physical robot manipulator (UR5e). Increasing the identification quality of previous DeLaN implementations that considered symmetrical linear friction models and did not consider the rotor inertia of the motors. In addition, our method demonstrated its robustness to different base fixture conditions. Globally, our work contributes with a DL architecture that can handle complex friction phenomena such as the NSCF, considering also viscous friction and rotor inertia of the motor.

The implementation of our method could lead to a improved alignment between the model and the real-world behaviour of the robot. Not only thanks to the adaptive nature of DL methods that allows models to adapt to non-linearities. Additionally, the data-driven and Lagrangian nature of our method makes it applicable for any holonomically constrained system, paving the way for agnostic dynamic model identification of other than serial robot architectures. The adoption of DeLaN+NSCF could open the door to a particular series of flexible and robust DL model-based controllers able to accurately compensate non-symmetric frictions. Therefore, offering better performances and improved control inputs that would lead to safer and precise movements.

Our aim is to study some of these model-based DL controllers and extend the complexity of DeLaN+NSCF to include the identification of more inertial and motor parameters of the robot. Additionally, our goal is to conduct our implementation with different robot architectures, to validate its agnostic capabilities for identification and model-based control. Furthermore, to thoroughly investigate the topic of excitation trajectories to generate optimal sets that are more DL-compatible. Moreover, our intention is to study model-based DL controllers for accurate and collaborative tasks.

ACKNOWLEDGMENT

We thank Dr. Arianna Traviglia and all the lab members of IIT@CCHT for allowing us to use their robot and lab to perform our experiments.

REFERENCES

[1] M. Lutter, C. Ritter, and J. Peters, “Deep lagrangian networks: Using physics as model prior for deep learning,” *7th International Conference on Learning Representations, ICLR 2019*, pp. 1–17, 2019.

[2] M. Gautier and S. Briot, *New Method for Global Identification of the Joint Drive Gains of Robots Using a Known Payload Mass*. 2011, ISBN: 9781612844558.

[3] M. Gautier and S. Briot, “Global identification of drive gains parameters of robots using a known payload,” in *2012 IEEE International Conference on Robotics and Automation*, 2012, pp. 2812–2817.

[4] S. Briot and M. Gautier, “Global identification of drive gains, dynamic parameters of parallel robots - part 2: Case study,” in *Romansy 19 – Robot Design, Dynamics and Control*, V. Padois, P. Bidaud, and O. Khatib, Eds., Vienna: Springer Vienna, 2013, pp. 93–100, ISBN: 978-3-7091-1379-0.

[5] M. Gautier and G. Venture, “Identification of standard dynamic parameters of robots with positive definite inertia matrix,” in *2013 IEEE/RSJ International Conference on Intelligent Robots and Systems*, 2013, pp. 5815–5820.

[6] A. Jubien, M. Gautier, and A. Janot, “Dynamic identification of the kuka lightweight robot: Comparison between actual and confidential kuka’s parameters,” in *2014 IEEE/ASME International Conference on Advanced Intelligent Mechatronics*, 2014, pp. 483–488.

[7] M. Lutter, K. Listmann, and J. Peters, “Deep lagrangian networks for end-to-end learning of energy-based control for under-actuated systems,” in *2019 IEEE/RSJ International Conference on Intelligent Robots and Systems (IROS)*, 2019, pp. 7718–7725.

[8] M. Lutter and J. Peters, “Combining physics and deep learning to learn continuous-time dynamics models,” *ArXiv*, vol. abs/2110.01894, 2021.

[9] Y. D. Zhong, B. Dey, and A. Chakraborty, “Symplectic ode-net: Learning hamiltonian dynamics with control,” *ArXiv*, vol. abs/1909.12077, 2019.

[10] J. K. Gupta, K. Menda, Z. Manchester, and M. J. Kochenderfer, “Structured mechanical models for robot learning and control,” *ArXiv*, vol. abs/2004.10301, 2020.

[11] M. A. Roehrl, T. A. Runkler, V. Brandtstetter, M. Tokic, and S. Obermayer, “Modeling system dynamics with physics-informed neural networks based on lagrangian mechanics,” vol. 53, Elsevier B.V., 2020, pp. 9195–9200.

[12] M. Gautier, S. Briot, and G. Venture, “Identification of consistent standard dynamic parameters of industrial robots,” in *2013 IEEE/ASME International Conference on Advanced Intelligent Mechatronics*, 2013, pp. 1429–1435.

[13] W Khalil and E Dombre, “Chapter 9 - dynamic modeling of serial robots,” in *Modeling, Identification and Control of Robots*, W Khalil and E Dombre, Eds., Oxford: Butterworth-Heinemann, 2002, pp. 191–233, ISBN: 978-1-903996-66-9.

[14] M Gautier and W Khalil, “Exciting trajectories for the identification of base inertial parameters of robots,” *The International Journal of Robotics Research*, vol. 11, pp. 362–375, 4 1992.

[15] F. Díaz Ledezma and S. Haddadin, “First-order-principles-based constructive network topologies: An application to robot inverse dynamics,” in *2017 IEEE-RAS 17th International Conference on Humanoid Robotics (Humanoids)*, 2017, pp. 438–445.

[16] Q. Leboutet, J. Roux, A. Janot, J. Rogelio, and G. Cheng, “Inertial Parameter Identification in Robotics: A Survey,” *Applied Sciences*, vol. 11, no. 9, p. 4303, May 2021.